Optical and Thermal Properties of Continuous Casting Mold Fluxes at Elevated Temperatures

H. Shibata, J.-W. Cho, T. Emi and M. Suzuki

Institute for Advanced Materials Processing
Tohoku University
2-1-1 Katahira, Aobaku, Sendai 980-77 Japan
+81-22-217-5144

ABSTRACT

Heat transfer from solidifying steel shell near the meniscus in continuous casting mold across infiltrated mold flux film to the mold was calculated with currently determined absorption and extinction coefficients, thermal diffusivities, and thermal interfacial resistances of the mold fluxes. Contribution of the conductive and radiative heat flux and interfacial resistance to the heat transfer was made clear for typical industrial mold fluxes. Calculated heat flux and its dependence on casting speed and steel grade showed a good agreement with plant observations.

1. INTRODUCTION

In continuous casting of steels into blooms and slabs, powder casting is exclusively used. Powder, which stands for mold flux in powder, granular or hollow spherical form, is a mixture of synthetic slag (CaO, MgO, SiO_2, Al_2O_3, TiO_2, ZrO_2, CaF_2), flux (NaF, CaF_2) and skeleton (C) materials. When the mold flux is added to the meniscus of steel melt in a hollow continuous casting mold, it melts to form a layer of molten slag, covered with unmelted layer of the flux as a thermal blanket, absorbs non-metallic inclusions surfacing from the melt, infiltrates the boundary between solidifying steel shell and the mold, and controls the lubrication and heat transfer at the shell/mold boundary.

The lubrication and heat transfer depend on the infiltrated slag film thickness which in turn is determined by the viscosity and solidifying point of the slag and the withdrawal (casting) speed of the castings. If the lubrication becomes insufficient and heat transfer excessive, a variety of surface cracks form, deteriorating further processings of the castings.

Recent developments in continuous casting of steel are toward higher casting speed and defect-free castings for direct rolling without surface conditioning. Higher casting speed makes, however, the slag film thickness thinner, resulting in an increased heat flux to the mold. Medium carbon steels subjecting to peritectic reaction are particularly sensitive to the crack formation under the increased heat flux, inhibiting the higher speed casting. Sustaining good lubrication at reduced heat flux is, therefore, one of the important objectives for designing the mold flux.

The slag film thickness may be increased by reducing the viscosity and solidifying point (ex. $\eta = 10^4$P) to such an extent that reasonable lubrication is secured. Reducing the heat flux at the same time is more difficult. Attempts have been made to control the chemistry of the mold flux and make the slag film partially crystalline to reduce radiative heat transfer. However, there is no consistent explanation available as yet on the factors controlling the heat transfer from the shell across the slag film to the mold, based on reliable optical and thermal data of the mold flux, and thermal interfacial resistance at the film/mold boundary.

This paper is intended to give an integrated analysis of the heat transfer with own determination of these properties, and examine the consistency with casting data obtained in industrial operations.

2. EXPERIMENTAL

Mold fluxes popularly used in major continuous casting plants in Japan for high speed casting of ultra low carbon (ULC1, ULC2), low carbon (LC1, LC2), and medium carbon (MC1, MC2, MC3, MC4) steels were selected and shown in Table 1 with their chemistry and physical properties. The mold fluxes, without the addition of the skeleton materials, were melted, quenched on a copper plate, annealed to remove thermal stress (glassy specimens), kept at 1073K for 1hr (crystalline specimens), ground and polished into a thin disc shape (9mm in diameter, 0.4-2.4mm in thickness).

Extinction and absorption coefficients for crystalline and glassy specimen were measured with an FTIR spectrometer in a high temperature cell. Thermal diffusivity was determined by a laser flash technique specifically developed to deal with thin film in glassy[1], crystalline or liquid phase[2] of these specimens. Thermal resistance at the slag film/mold boundary was evaluated by a transient temperature measurement[3] in a copper plate on which the slag melts were cast.

3. RESULTS

Thermal diffusivity of slag films in glassy, crystalline and liquid state of the mold fluxes given in Table 1 is partly reproduced from our previous work[3] in Figs. 1 and 2. Convincingly, the thermal diffusivity (and its variation) of the crystalline state is larger than that of the glassy state, decreases with temperature, approaching as temperature increases to $4\sim6 \times 10^{-7}m^2s^{-1}$ which is similar to that of the glassy state. The thermal diffusivity of liquid slag film is almost the same as that for the glassy one.

The absorption coefficient and extinction coefficient of infrared light are given for glassy and crystalline slag films in Figs. 3-4. As reported elsewhere[4,5], there is a window at 2.0~4.6μm range where the absorption coefficient is less than $1000m^{-1}$ for all the glassy slag films. The extinction coefficient becomes naturally much larger, ca. 10000-$30000m^{-1}$, for the crystalline films due to the scattering at the grain boundaries. The absorption and extinction

Table.1 Chemical compositions (in wt.%) and physical properties of mold fluxes used

Mold flux	ULC1	ULC2	LC1	LC2	MC1	MC2	MC3	MC4
Steel grade applied	Ultra low carbon		Low carbon		Medium carbon			
SiO_2	30.1	39.7	30.5	35.0	34.0	31.8	33.4	33.1
CaO	35.0	32.4	32.6	33.8	43.7	44.8	40.8	43.2
Al_2O_3	5.3	6.0	2.5	6.4	3.0	3.7	8.2	5.6
Fe_2O_3	1.5	0.8	1.3	0.7	0.4	0.4	-	-
Na_2O	3.6	9.7	13.0	11.2	6.6	7.3	9.1	9.4
MgO	6.8	2.4	1.5	2.3	5.1	1.9	-	-
MnO	2.3	0.1	6.0	0.1	-	0.1	-	-
TiO_2	4.7	0.1	-	0.1	-	0.1	-	-
K_2O	-	0.7	-	0.5	-	0.3	-	-
B_2O_3	5.7	-	-	-	-	-	-	-
Li_2O	-	5.5	3.1	4.6	-	3.9	2.0	2.2
F	5.9	5.0	10.8	8.4	8.8	9.9	11.2	9.4
CaO/SiO_2	1.16	0.82	1.07	0.96	1.29	1.41	1.22	1.30
Viscosity (Pa·s at 1573K)	0.15	0.20	0.04*	0.09	0.18	0.05	0.11	0.11
Softening point(K)	1253	1228	1243	1203	1413	1303	-	-
Solidifying point(K)	1193	-	1353	-	1473	-	1383	1398
Crystallization temperature(K)	-	1253	-	1303	-	1428	-	-

*Rotary type viscometer

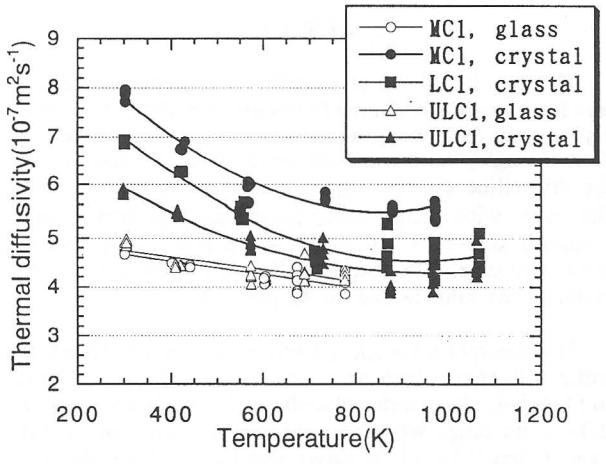

Fig. 1 Thermal diffusivity of glassy and crystalline mold fluxes.

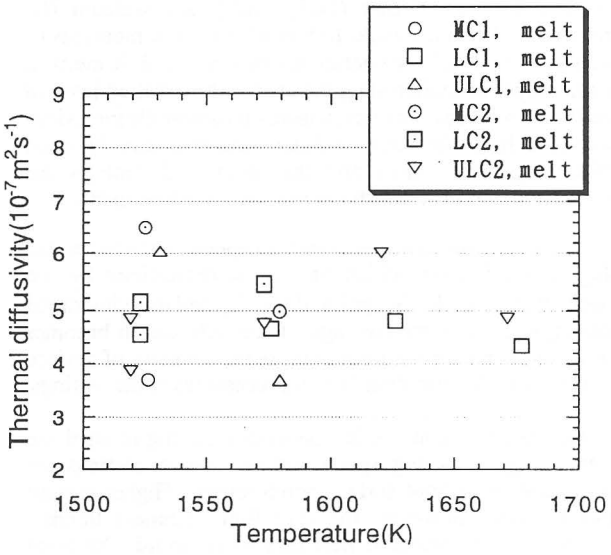

Fig. 2 Thermal diffusivity of liquid mold fluxes.

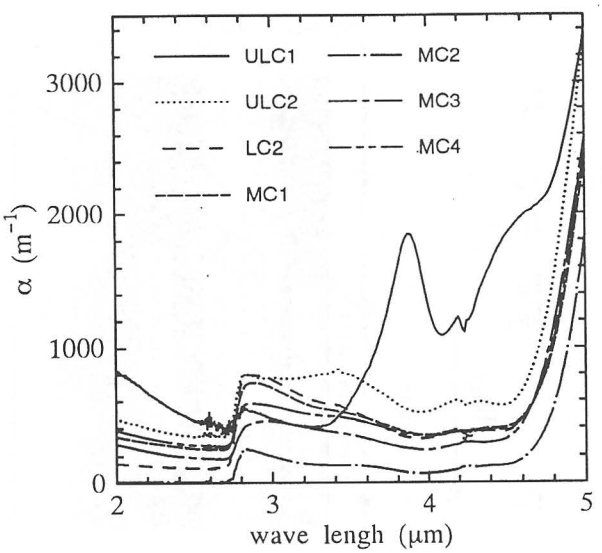

Fig. 3 Absorption coefficient of glassy mold fluxes at room temperature.

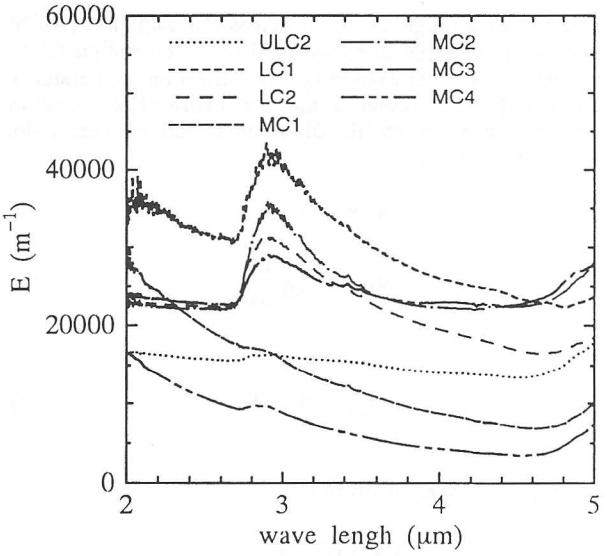

Fig. 4 Extinction coefficient of crystalline mold fluxes at room temperature.

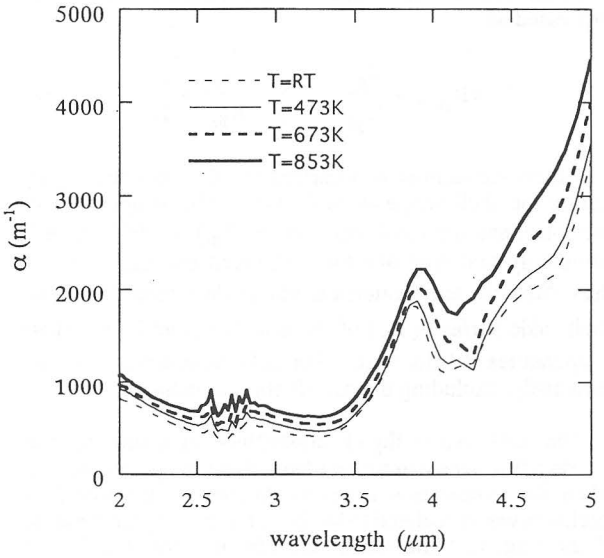

Fig. 5 Absorption coefficient of glassy mold flux (ULC1) at elevated temperatures.

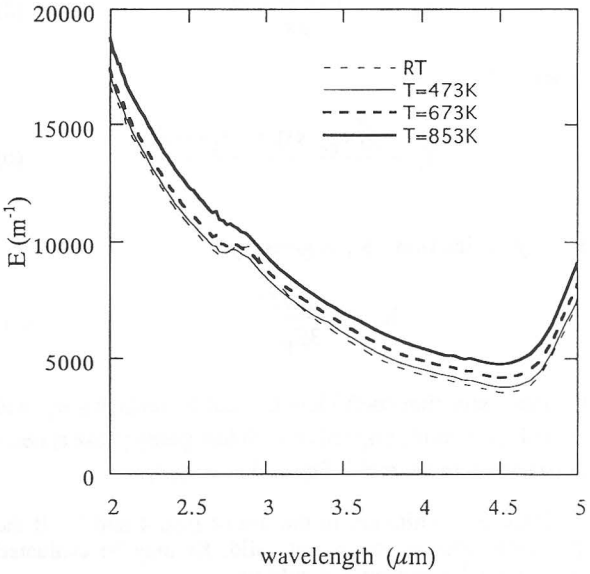

Fig. 6 Extinction coefficient of crystalline mold flux (MC4) at elevated temperatures.

coefficients are not much influenced by the chemistry of the slag film within the range presently investigated. Also, the two coefficients do not change with temperature, as shown in Figs. 5 and 6, for both glassy and crystalline films.

The thermal resistance at the slag film/mold boundary has been determined in our previous work[3] to be 5-10cm^{2}WK^{-1}, increasing with the size of cells which form surface roughness of the slag film in contact to the mold.

4. DISCUSSION

Heat flux 30mm below the meniscus of steel melt in the mold, where early stage of shell formation and occurrence of surface cracks in the solidifying shell are considered to take place, is calculated on the basis of the data given in the previous section.

A model to represent the meniscus area is shown in Fig. 7. Heat transfers in conductive and radiative modes from

liquid steel through the shell across the slag film [which may be divided into three layers, liquidus, crystalline (slow cooled to the level exceeding crystallization temperature), and glassy (rapid cooled to the level below glass transition temperature) layer] and the film/mold boundary to the mold, and hence one has

$$q_t = q_c + q_r \tag{1}$$

$$q_t = -K_{eff}\frac{dt}{dx} \tag{2}$$

where

$$K_{eff} = K_c + K_r \tag{3}$$

For liquid film, K_r is given by

$$K_r = \frac{n^2\sigma\,(T_{fs}^4 - T_c^4)}{0.75\alpha_p d_{liq.} + \frac{1}{\varepsilon_{mw}} + \frac{1}{\varepsilon_{sw}} - 1}\,\frac{d_{liq.}}{T_{fs} - T_c} \tag{4}$$

with apparent absorption coefficient defined[9] as

$$\alpha_p = -\frac{\partial\,[\log T_r\,(x)]}{\partial x} \tag{5}$$

where

$$T_r = \frac{\int_0^\infty e_{b\lambda}\,\exp(-\alpha_\lambda x)\,d\lambda}{e_b} \tag{6}$$

For crystalline film, K_r is given by

$$K_r = \frac{16n^2\sigma T^3}{3E_p} \tag{7}$$

with the extinction coefficient E_λ and E_p replacing α_λ and α_p in Eqs. 5 and 6, respectively. When glassy phase appears in contact with the mold, Eqs. 4-6 also apply.

There is a limitation in the use of Eqs. 4 and 7. If the grey body assumption is not valid, Kr may be evaluated excessively larger than it should be.

Table 2 Conditions employed for calculating heat flux.

Steel grade	Low carbon	Medium Carbon
Casting speed	2.0 m·min^{-1}	1.6 m·min^{-1}
K_S	32.1 W·m^{-1}·K^{-1}	31.6 W·m^{-1}·K^{-1}
T_S	1783K	1753K
Applied flux	LC2	MC1
C_p[7]	1230 J·kg^{-1}K^{-1}	
ρ[7]	2712 kg·m^{-3}	

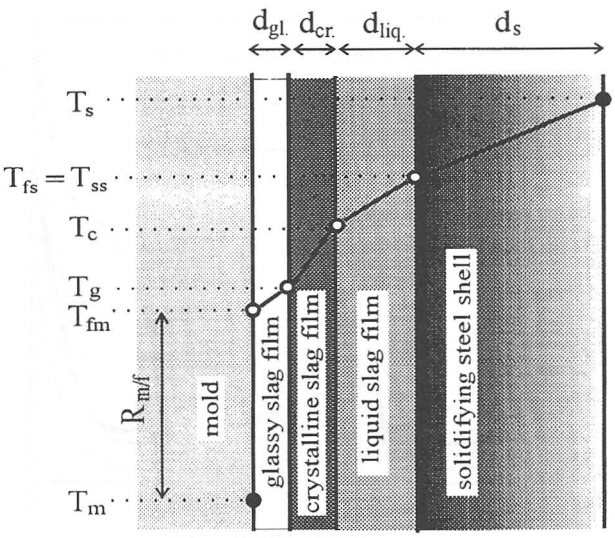

Fig. 7 Schematic of solidifying shell/mold boundary with infiltrated slag film with liquid, crystalline and glassy layers.

In the above, total conductive thermal resistance can be expressed as

$$R_t = R_{m/f} + \frac{d_{gl.}}{K_{gl.}} + \frac{d_{cr.}}{K_{cr.}} + \frac{d_{liq.}}{K_{liq.}} + \frac{d_s}{K_s} \tag{8}$$

Actual calculation was carried out first to obtain q_c by setting the shell temperature (T_s) at solidus temperature of each steel and the mold temperature (T_m) at 593K which is commonly practiced one for high speed casting. With q_c thus obtained, temperatures at mold side surface (T_{fm}) and shell side surface (T_{fs}) of the slag film, and intermediate temperatures at different positions in between were calculated tentatively, excluding the contribution of radiation.

The thickness of liquid, crystalline-, or glassy-layer in the slag film was determined from these temperatures, eg., when the temperature for some fraction of the slag film thickness was calculated to be above the melting temperature of the slag, that fraction of the film was taken to be the liquid layer. Here, the thickness of the slag film has been given from plant observation as a function of the casting speed as 0.3mm at 1.6m·min^{-1} for medium carbon peritectic steel and 0.2mm at 2.0m·min^{-1} for low carbon steel[9].

Second, radiation heat flux was approximately evaluated by calculating radiative heat transfer between the two sides of each layer with temperatures calculated in the above and with Eqs. 4 and 7.

This q_r was then added on the calculated q_c, and resulting tentative $q_t = (q_r + q_c)$ was used to recalculate T_{fm}, T_{fs} and the intermediate temperatures with $K_{eff} = K_c + K_r$. This calculation was repeated until q_t converged. In calculating the thickness of each layer, existence of the glassy layer was excluded since T_{fm} became

very close to the crystallization temperature. Then, the thickness ratio of the liquid to crystalline layer was varied in the previous converging calculation until the calculated intermediate temperature agreed with the solidifying point of the slag film.

The results of the calculations are summarized in Fig. 8. Here circle marks represent the case where the thickness, d_s (mm), of solidifying steel shell grows at $20\sqrt{t\,(\text{min.})}$, whereas square marks show the growth at $25\sqrt{t\,(\text{min.})}$. Also, filled marks are for slag film totally in liquid phase with emissivity of the mold side of the film taken to be 0.7, and open marks are for the same with the emissivity 0.4. Concentric double circle mark and double square one are, respectively, for the slag film consisting of crystallized layer and liquid layer. The marks at casting speed of 1.5 m·min^{-1} are for mold flux MC-1 in Table 1 used for casting crack sensitive medium carbon peritectic grade, and those at 2.0m·min^{-1} are for LC-2 for low carbon grade. Grey and white bars in the figure indicate critical heat flux beyond which surface cracks occurred on the medium and low carbon grade even in well standardized plant operation[8].

It is interesting to note that the calculated heat flux falls just below the critical value, increases from 1.5 to 1.7 × 10^{6}W·m^{-2} as the casting speed increases from 1.6 to 2.0m·min^{-1}. As shown in Table 2, this range of heat flux agrees well with plant observation for casting these grades of steels without surface cracks.

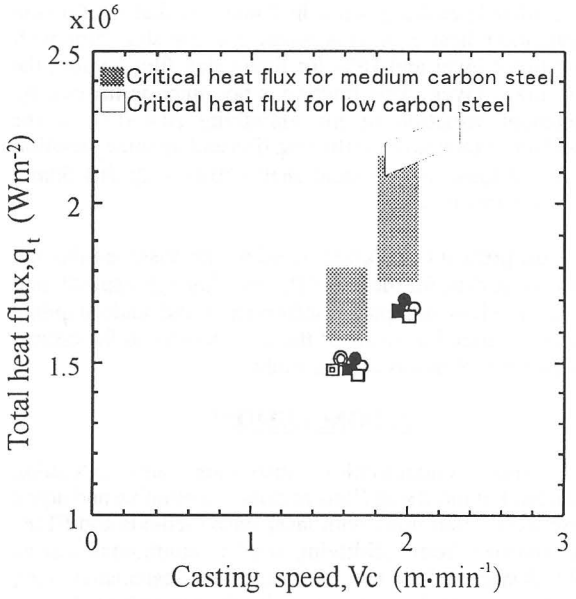

Fig. 8 Calculated heat flux from shell to mold in comparison with plant observation (symbols correspond to those given in Tables 3-5).

Table 3 Calculated heat flux and fraction of radiative heat flux for 0.3mm slag film with crystallized layer ($\varepsilon_{mw} = 0.7$, $\varepsilon_{sw} = 0.78$).

ds(mm)	symbol	layer	Kc (Wm^{-1}K^{-1})	Kr (Wm^{-1}K^{-1})	q_t (Wm^{-2})	q_r/q_t(%)
2.74	◎	crystal (0.1mm)	1.83	0.096	1.51×10^{-6}	5
		liquid (0.2mm)	1.33	0.232		15
3.42	◻	crystal (0.1mm)	1.83	0.092	1.47×10^{-6}	5
		liquid (0.2mm)	1.33	0.220		14

Table 4 Calculated heat flux and fraction of radiative heat flux for 0.3mm liquid slag film with different emissivities (MC1, $V_c = 1.6$m·min^{-1}).

ds(mm)	symbol	ε_{mw}	Kc (Wm^{-1}K^{-1})	Kr (Wm^{-1}K^{-1})	q_t (Wm^{-2})	q_r/q_t(%)
2.74	○	0.4	1.33	0.197	1.48×10^{-6}	13
	●	0.7	1.33	0.317		19
3.42	□	0.4	1.33	0.187	1.51×10^{-6}	12
	■	0.7	1.33	0.301		18

Table 5 Calculated heat flux and fraction of radiative heat flux for 0.3mm liquid slag film with different emissivities (LC2, $V_c = 2.0$m·min^{-1}).

ds(mm)	symbol	ε_{mw}	Kc (Wm^{-1}K^{-1})	Kr (Wm^{-1}K^{-1})	q_t (Wm^{-2})	q_r/q_t(%)
2.45	○	0.4	1.33	0.152	1.69×10^{-6}	10
	●	0.7	1.33	0.248	1.67×10^{-6}	16
3.06	□	0.4	1.33	0.145	1.65×10^{-6}	10
	■	0.7	1.33	0.232	1.62×10^{-6}	15

Another interesting result in Table 2 is that the fraction of radiation heat flux is a small 5% for slag film with crystallized layer and 18% for liquid slag film without the crystallized layer. This fraction is not much influenced by substantial variation in the emissivity (0.4~0.7) of the boundary of each layer of the slag film and by some variation in the thickness of the steel shell ($20\sqrt{t}$ ~ $25\sqrt{t}$) 30mm below the meniscus.

Thus, present calculation based on the observed thermal and optical data for the mold fluxes, although approximate in nature, gives acceptable information and understanding on the integrated analysis of the heat transfer in the critical area in the continuous casting mold.

5. CONCLUSIONS

Thermal conductivities, absorption and extinction coefficient of mold slag films in glassy, crystalline and liquid phase were determined with laser flash methods and FTIR. Heat transfer from solidifying shell to continuous casting mold 30mm below the meniscus was calculated semi empirically with these data, previously determined thermal interfacial resistance at the slag film/mold boundary, and observed film thickness in plant operation. The calculated heat flux agreed well with observation in plant operation, increasing with casting speed from $1.5\times10^{6}W\cdot m^{-2}$ at $1.6m\cdot min^{-1}$ to $1.7\times10^{6}W\cdot m^{-2}$ at $2.0m\cdot min^{-1}$. Radiative heat flux is found to be 5~19% of total, decreasing from about 15% to 5% when crystallized layer is formed in the slag film.

ACKNOWLEDGMENT

The authors wish to thank Nippon Steel Co., Sakai Chemical Industry Co., and Shinagawa Refractories Co. Ltd. for providing us with the mold flux specimens.

REFERENCES

1. H. Shibata, T. Emi, Y. Waseda, K. Kondo, H. Ohta, and K. Nakajima, "Thermal Diffusivities of Continuous Casting Mold Fluxes for Steel in the Glassy and Crystalline States", Tetsu-to-Hagane, Vol. 82, 1996, pp. 504-508

2. H. Ohta, M. Masuda, K. Watanabe, K. Nakajima, H. Shibata, and Y. Waseda, "Determination of Thermal Diffusivities of Continuous Casting Powders for Steel by Precisely Excluding the Continuous of Radiative Component at High Temperature", Tetsu-to-Hagane, Vol. 80, 1994, pp. 463-468

3. H. Shibata, K. Kondo, M. Suzuki, and T. Emi, "Controlling in-Mold Heat Transfer in Continuous Casting by Trimming the Properties of Mold Flux Film at Shell/Mold Boundary", ISIJ Internat. Suppl., Vol. 36, No. 12, 1996 in press.

4. H. Ohta, K. Watanabe, K. Nakajima, and Y. Waseda, "Absorption Coefficient of Continuous Casting Powder for Steel", High Temperature Materials and Processes, Vol. 12, 1993, pp. 139-142

5. M. Susa, K. Nagata, and K. C. Mills, "Absorption Coefficients and Refractive Indices of Synthetic Glassy Slags Containing Transition Metal Oxides", Ironmaking and Steelmaking, Vol. 20, 1993, pp. 372-378

6. Y. Nagano and E. Takeuchi, "Mould and Mould Flux for High Speed Continuous Casting", CAMP-ISIJ, Vol. 1, 1988, pp. 146-149

7. R. Taylor and K. C. Mills, "Physical Properties of Casting Powders : Part 3 Thermal Conductivities of Casting Powders", Ironmaking and Steelmaking, Vol. 15, 1988, pp. 187-194

8. S. Hiraki, K. Nakajima, T. Murakami, and T. Kanazawa, "Influence of Mold Heat Fluxes on Longitudinal Surface Cracks During High Speed Continuous Casting of Steel Slab", Steelmaking Conf. Proc., Vol. 77, 1994, pp. 397-403, Iron and Steel Soc., Warrendale, PA

NOMENCLATURE

c_p = specific heat of flux
d = thickness of slag
E = extinction coefficient
e = emissive power
K = thermal conductivity
n = refractive index
q = heat flux
$R_{m/f}$ = thermal interfacial resistance between mold and slag
R_t = total thermal resistance between mold and steel melt
T_c = solidifying point of flux
T_{fm} = temperature of slag film surface in contact with copper mold
T_{fs} = temperature of liquid slag film surface in contact with solidifying steel shell
T_g = crystallization temperature of flux
T_m = temperature of mold surface
T_{ss} = temperature of solidifying steel shell in contact with slag film
V_c = casting speed
α = absorption coefficient
ε_{mw} = emissivity of mold side surface
ε_{sw} = emissivity of solidifying steel shell in contact with slag film
ρ = density of flux
σ = Stefan-Boltzmann constant

Subscripts

b = black body
c = conduction
cr. = crystalline slag film
eff = effective
gl. = glassy slag film
liq. = liquid slag film
p = apparent
r = radiation
s = solidifying steel shell
λ = wave length